

# PCCP

Accepted Manuscript



This is an *Accepted Manuscript*, which has been through the Royal Society of Chemistry peer review process and has been accepted for publication.

*Accepted Manuscripts* are published online shortly after acceptance, before technical editing, formatting and proof reading. Using this free service, authors can make their results available to the community, in citable form, before we publish the edited article. We will replace this *Accepted Manuscript* with the edited and formatted *Advance Article* as soon as it is available.

You can find more information about *Accepted Manuscripts* in the [Information for Authors](#).

Please note that technical editing may introduce minor changes to the text and/or graphics, which may alter content. The journal's standard [Terms & Conditions](#) and the [Ethical guidelines](#) still apply. In no event shall the Royal Society of Chemistry be held responsible for any errors or omissions in this *Accepted Manuscript* or any consequences arising from the use of any information it contains.

# Aromatic Stabilization of Functionalized Corannulene Cations

Jingbai Li, Andrey Yu. Rogachev\*

*Department of Chemistry, Illinois Institute of Technology, Chicago, IL 60616, USA*

To whom correspondence should be addressed:

E-mail: [andrey.rogachev@gmail.com](mailto:andrey.rogachev@gmail.com) and/or [andrey.rogachev@iit.edu](mailto:andrey.rogachev@iit.edu) (A. Yu. Rogachev)

## Abstract

The first comprehensive theoretical investigation of aromaticity in functionalized corannulene cations of general formula  $[\text{CH}_3\text{-C}_{20}\text{H}_{10}]^+$  was accomplished. The experimentally known system  $[\text{CH}_3\text{-hub-C}_{20}\text{H}_{10}]^+$  was augmented by two other possible isomers, namely, *rim*- and *spoke*-ones. Changes in aromaticity, when going from neutral corannulene to its functionalized cations, were monitored with help of descriptors of different nature such as structure-based HOMA, topological PDI and FLU, and magnetic NICS. Highly efficient tool for analysis and visualization of delocalization and conjugation named ACID was also utilized. In a final step, a complete set of  $^1\text{H}$  and  $^{13}\text{C}$  chemical shifts was calculated and compared with available experimental data. Conservation of aromaticity of 6-membered rings along with vanishing anti-aromatic character of central 5-membered ring was found to be the main reason for exceptional stability of *hub*-isomer. At the same time, functionalization of corannulene moiety at *rim*- or *spoke*-site resulted in dramatic elimination of aromaticity of 6-membered rings, whereas anti-aromatic character of the central ring remained. Altogether, it led to much lower stability of these isomers in comparison with that of *hub*-one.

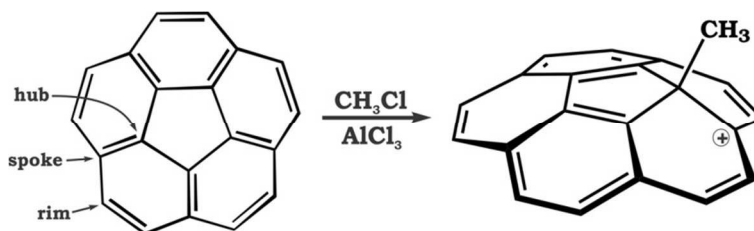
## Introduction

During the last 40 years, the chemistry of carbon rich compounds evolved dramatically. The discovery of fullerenes in 1985<sup>1</sup> and the accompanied discovery of endohedral metallofullerenes,<sup>2</sup> which encapsulate an (metal) atom(s) into its spherical space inside the carbon cage, gave rise to the research and discovery of various types of carbon nanostructures. A related class of three-dimensional carbon surfaces, carbon nanotubes, was prepared in 1991 by using a reactor similar to the one used for the mass production of C<sub>60</sub>.<sup>3</sup> Single-wall carbon nanotubes (SWNT) show favorable properties like high thermal conductivity and other fascinating mechanical<sup>4</sup> and electrical properties.<sup>5</sup> The latest groundbreaking discovery was made at the beginning of this century, when Geim and Novoselov succeeded in extracting single-atom-thick crystallites (graphene) from bulk graphite in 2004.<sup>6</sup>

Open-geodesic polyaromatic hydrocarbons mapping onto the surface of fullerenes (and therefore often referred to as buckybowls or fullerene fragments) represent another unique class of non-planar conjugated molecules.<sup>7</sup> In contrast to the planar graphene and closed-cage fullerenes, they possess built-in curvature and strain and have two non-equivalent  $\pi$ -surfaces, concave and convex, that are readily accessible. This class of bowl- and basket-shaped polyarenes is growing rapidly due to increasing efforts of several organic chemistry groups.<sup>8</sup> As a result, buckybowls with curvature greater than that in C<sub>60</sub>-fullerene have recently been synthesized,<sup>9</sup> but their properties and reactivity remain largely unexplored. Potential applications of these unusual molecules range from rational design of fullerenes, nanotubes and their endohedral compounds to supramolecular architectures, for they can act as molecular clips and tweezers<sup>10</sup> or even potential materials for new-type Li-batteries.<sup>11</sup>

In contrast to well-developed chemistry of exterior part of polyaromatic hydrocarbons (so-called *rim*-bonds, Scheme 1),<sup>7,12,13,14</sup> the interior part of polyaromatic hydrocarbons is believed to be inert with respect to functionalization. For instance, derivatives of pyrene that bear substituents attached to the interior carbon atoms are known, but these have been constructed by multi-step syntheses and cannot be obtained directly from pyrene.<sup>15</sup> The main reason for it is that when the substituent is attached to the interior carbon atom, it destroys the aromatic conjugation in all rings it belongs. The loss of benzenoid aromaticity associated with formation of such covalent bonds clearly contributes to the reluctance of PAH to react at its interior carbon atom. The same situation was observed for curved PAH systems until recently. In 2011 the group of Petrukhina successfully synthesized and crystallized first corannulene cations [R-*hub*-C<sub>20</sub>H<sub>10</sub>]<sup>+</sup> (R=CH<sub>3</sub>, CH<sub>2</sub>Cl, CHCl<sub>2</sub>, CCl<sub>3</sub>) functionalized at interior space<sup>16</sup> (Scheme 1). It was found that these cations are formed under relatively mild conditions of Friedel-Crafts reaction. Subsequent theoretical study<sup>17</sup> helped to identify two main reasons for stability of such cations, namely, relief of strain energy and conservation of aromaticity, which resulted in complete delocalization of positive charge of R<sup>+</sup> over the whole polyaromatic surface. At the same time, under the same circumstances C<sub>60</sub> and C<sub>70</sub> fullerenes give only the products of 1,4-addition of halogenated hydrocarbon, albeit having even more curved surface.<sup>18</sup> It should be noted that the products of addition of transient carbocations such as CCl<sub>2</sub><sup>+</sup> and CCl<sub>3</sub><sup>+</sup> to the corannulene interior have been identified in solution mixtures based on <sup>1</sup>H NMR studies back in 1999,<sup>19</sup> however, no structural data were provided.

## Scheme 1



In this article, we report the first comprehensive theoretical investigation of changes in aromaticity of bowl-shaped systems, when going from neutral unperturbed molecule of corannulene ( $\text{C}_{20}\text{H}_{10}$ ) to its cationic derivative, functionalized at interior carbon atom. For the sake of comparison, the set of systems considered was augmented by two other possible isomers, functionalized at *rim*- and *spoke*-carbon atoms (Scheme 1). These isomers were previously found to be less energetically preferable (or in other words, less stable) than *hub*-functionalized cation,<sup>17</sup> explaining their absence in experiment. Detailed study of aromaticity included calculations of a set of popular descriptors, such as structure-based harmonic oscillator model of aromaticity (HOMA), aromaticity electronic criteria based on Bader's topological quantum theory *para*-delocalization index (PDI) and aromatic fluctuation index (FLU), and nucleus-independent chemical shift (NICS). The study was complemented by detailed investigation of magnetic induced ring current using anisotropy of the induced current density approach (ACID). At the final step, the complete set of chemical shifts for all hydrogen and carbon atoms was calculated and compared with available experimental values.

## Calculation details

Geometry optimizations were performed at the DFT level of theory with the help of PBE0<sup>20</sup> hybrid correlation-exchange functional. All atoms were described by correlation-consistent basis sets of triple- $\zeta$  quality (cc-pVTZ). In all cases, no symmetry restrictions were applied. All calculated structures correspond to local minima (no imaginary frequencies) on the corresponding potential energy surfaces, as determined by calculation of the full Hessian matrix, followed by estimation of frequencies in the harmonic approximation. All these calculations were performed using the Firefly program (version 8.1.0).<sup>21</sup>

Optimized geometries were then used to get insights into the electronic structure of target systems in terms of natural bond orbitals (NBO).<sup>22</sup> Bond orders quoted are those from the Wiberg formulation<sup>23</sup> (Wiberg bond indices) incorporated in the NBO analysis. All computations were performed with NBO<sup>24</sup> (version 6.0) program.

**Aromaticity descriptors.** Using PBE0/cc-pVTZ-optimized geometries, a set of theoretical descriptors/indexes of aromaticity was calculated. Brief description of all used techniques is given below.

*Harmonic Oscillator Model of Aromaticity (HOMA).* HOMA approach is based on the normalized deviation of a given bond length ( $R_i$ ) from the optimal aromatic value ( $R_{opt}=1.388\text{\AA}$  in benzene, here optimized at the same PBE0/cc-pVTZ level of theory), defined by Kruszewski and Krygowski<sup>25</sup> as:

$$HOMA = 1 - \frac{\alpha}{n} \sum_{i=1}^n (R_{opt} - R_i)^2,$$

where  $n$  is the number of bonds considered and  $\alpha$  (in our case is equal to 257.7) is the normalization coefficient to give HOMA = 0 for a nonaromatic system and HOMA = 1 for a system with all bonds equal to the bonds of a given optimal aromatic system.

The local aromaticity as well as anti-aromaticity in the selected series is assessed by *Nuclear Independent Chemical Shift* (NICS) calculations.<sup>26</sup> The NICS values here are theoretical chemical shifts of ring centers in cyclic or polycyclic compounds (so-called NICS(0), although it can be calculated at any point of space). This approach was introduced by von Rague Schleyer *et al.* as a simple and very efficient probe for local aromaticity. To match the familiar NMR convention, the NICS indices correspond to the negative of the magnetic shielding computed at chosen points in the vicinity of molecules. The significantly negative (*i.e.* magnetically shielded) NICS values at interior positions of rings or cages indicate the presence of induced diatropic ring currents or “aromaticity”, whereas the positive values (*i.e.* deshielded) at each point denote paratropic ring current and “anti-aromaticity”. In spite of being highly debated parameter,<sup>27</sup> NICS (in its NICS(0) version) seems to be a balanced descriptor in the case of curved polyaromatic systems decorated at convex interior face. All these calculations were performed using Gauge Independent Atomic Orbitals (GIAO) approach with help of Gaussian 09 program<sup>28</sup> at the PBE0/cc-pVTZ level of theory.  $^1\text{H}$  and  $^{13}\text{C}$  NMR chemical shifts were also calculated at this level of theory.

*Para-Delocalization Index (PDI) and Aromatic Fluctuation Index (FLU)*. PDI<sup>29</sup> and FLU<sup>30</sup> descriptors are based on topological Quantum Theory of Atom in Molecule (QTAIM)<sup>31</sup> approach. The *PDI* is a specific measure of aromaticity for six-membered ring, in which there are three para-related positions, and is defined as:

$$PDI = \frac{\delta(1,4) + \delta(2,5) + \delta(3,6)}{3}$$

where  $\delta(1,4)$ ,  $\delta(2,5)$  and  $\delta(3,6)$  are the delocalization index of *para* site atom pairs. Obviously, PDI indicates the strength of the delocalization of electrons around a ring, namely, greater PDI values denote greater aromaticity.

The *FLU index* was constructed by following the HOMA philosophy, which measures the divergence of a given molecule to optimal aromatic molecule (here benzene, optimized at the same level) by using delocalization index of each bond and localization index of atom in bond pair. Therefore, lower FLU value corresponds to stronger aromaticity. The FLU formula<sup>30</sup> was given as:

$$FLU = \frac{1}{n} \sum_{A-B}^{RING} \left[ \left( \frac{V(A)}{V(B)} \right)^\alpha \left( \frac{\delta(A,B) - \delta_{ref}(A,B)}{\delta_{ref}(A,B)} \right) \right]^2,$$

where the summation runs over all adjacent pairs of atoms in the ring,  $n$  is the number of atoms of the ring.  $V(A)$  and  $V(B)$  are the global delocalization of atom A and B or so-called valence electrons,  $\delta(A, B)$  and  $\delta_{ref}(A, B)$  are the delocalization index of atom A and B and its reference value, respectively.  $\alpha$  is used to ensure the ration of atomic valences is greater than 1, defined as:

$$\alpha = \begin{cases} 1 & V(B) > V(A) \\ -1 & V(B) \leq V(A) \end{cases}$$

To calculate delocalization and localization index, the exchange-correlation density of a given molecule was first integrated over the atomic space, which could be defined by different partition of space. The integral will produce a density matrix where the matrix elements, therefore, are delocalization index off diagonal and localization index in diagonal. In our case, two types

atomic space were tested: (i) AIM, using Bader's atomic basin definition,<sup>32</sup> (ii) and Fuzzy atomic space, using Becke atomic space definition.<sup>33</sup> The correlation between the results calculated in fuzzy atomic space and in AIM atomic space was previously reported to be excellent.<sup>34</sup> All QTAIM calculations were carried out by Multiwfn 3.3.7 program.<sup>35</sup>

**Aromatic Ring Current.** Magnetic induced ring current of corannulene molecule and cations were calculated by using Anisotropy of the Induced Current Density (ACID) approach.<sup>36</sup> The applied magnetic field is perpendicular to the five-membered ring. To obtain induced current vectors and plot map, ACID 2.0.0 program uses the current density tensors, calculated by Continuous Set of Gauge Transformations (CSGT) method<sup>37</sup> implemented in Gaussian 09 package.

## Results and discussion

The classical way to define aromaticity is the manifestation of the following features of cyclic  $\pi$ -conjugated molecules:<sup>38</sup> (i) structural – reduced bond length alternation or bond equalization as compared to their acyclic unsaturated analogues (consequence of delocalization), (ii) energetic – an enhanced stability (large resonance energy), (iii) chemical behavior – a tendency to retain their  $\pi$ -electron structure in chemical reactions (electrophilic aromatic substitution), (iv) magnetic – the induction of a diatropic ring current by an external field resulting in anomalous chemical shift, large magnetic anisotropy, and diamagnetic susceptibility exaltation. In this study, we will mainly be focused on structural,  $\pi$ -electron delocalization, and magnetic aspects of aromaticity.

### I. Structural aspects

Our previous theoretical consideration<sup>17</sup> revealed that all possible isomers of functionalized corannulene cations, namely, *hub*-, *rim*-, and *spoke*-ones, correspond to the minima on potential energy surface. However, only *hub*-isomer was observed experimentally and its crystal structure was determined. In this part, the structural changes in  $[\text{CH}_3\text{-C}_{20}\text{H}_{10}]^+$  systems will be investigated in comparison with those in unperturbed neutral corannulene. Selected calculated geometrical parameters for all systems considered are summarized in Table 1, whereas equilibrium geometries are depicted in Fig. 1.

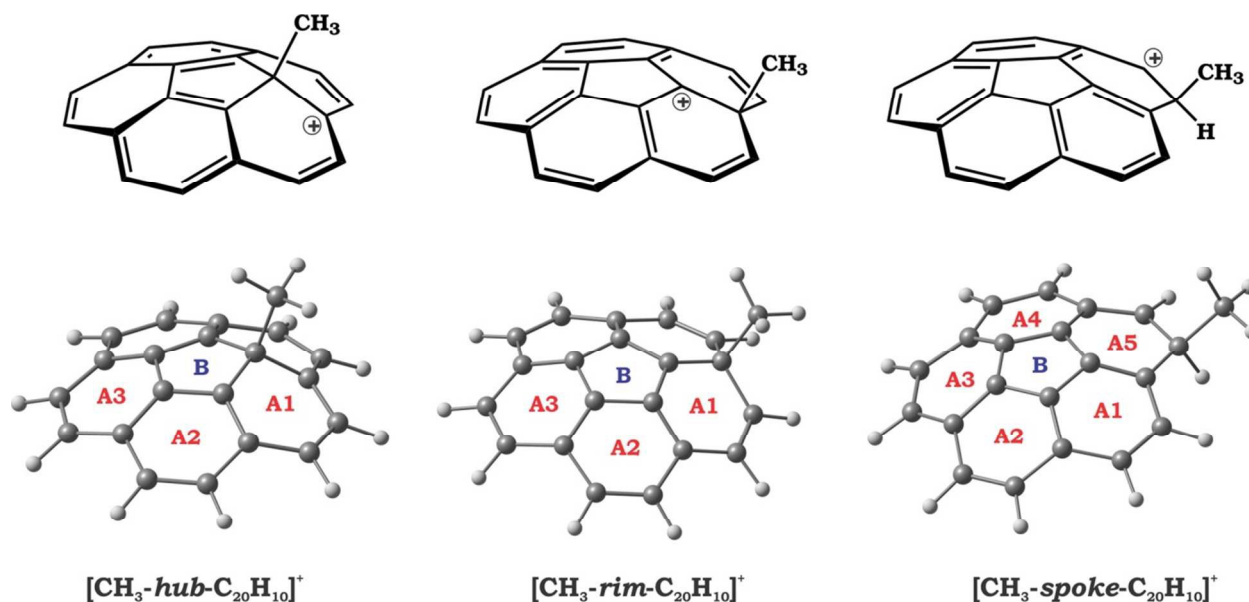
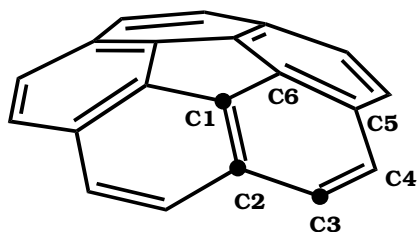


**Figure 1.** ChemDraw representation of all studied functionalized corannulene cations along with equilibrium geometries (PBE0/cc-pVTZ) and aromatic ring labeling scheme (only for symmetry unique rings).

**Table 1.** Selected geometrical and electronic structure parameters for all  $[\text{R-C}_{20}\text{H}_{10}]^+$  systems considered along with atom labeling scheme (PBE0/cc-pVTZ) as well as for the group of reference molecules ( $\text{C}_6\text{H}_6$ ,  $\text{C}_5\text{H}_5^-$ ,  $\text{C}_5\text{H}_6$ ).



Parameter	$\text{C}_6\text{H}_6$	$\text{C}_5\text{H}_5^-$	$\text{C}_5\text{H}_6$	$\text{C}_{20}\text{H}_{10}$	$[\text{CH}_3\text{-hub-C}_{20}\text{H}_{10}]^+$	$[\text{CH}_3\text{-rim-C}_{20}\text{H}_{10}]^+$	$[\text{CH}_3\text{-spoke-C}_{20}\text{H}_{10}]^+$
C-C'					1.570	1.553	1.600
C1-C2	1.388	1.407	1.493	1.376	1.477	1.364	1.446

C2-C3			1.342	1.438	1.406	1.505	1.509
C3-C4			1.460	1.380	1.396	1.502	1.352
C4-C5			1.342	1.438	1.428	1.376	1.451
C5-C6				1.380	1.377	1.403	1.383
C6-C1				1.409	1.481	1.417	1.403
b.o. C-C'					0.90	0.96	0.86
b.o. C1-C2	1.44	1.41	1.05	1.34	0.99	1.40	1.05
b.o. C2-C3			1.82	1.22	1.35	1.02	0.99
b.o. C3-C4			1.13	1.63	1.49	1.07	1.78
b.o. C4-C5			1.82	1.22	1.24	1.52	1.15
b.o. C5-C6			1.05	1.34	1.33	1.19	1.31
b.o. C6-C1				1.19	0.98	1.15	1.24

Bond lengths are in Å, bond orders are Wiberg bond indices. C' denotes the carbon atom of methyl group attached to the corannulene bowl. Bold dots in the scheme represent the carbon atoms of attachment in the bowl moiety corresponding to *hub*-, *spoke*-, and *rim*-isomers.

In parent C<sub>20</sub>H<sub>10</sub>, all five six-membered rings are known to show aromatic behavior, whereas the central 5-membered ring possesses significant anti-aromatic character.<sup>7,31,39</sup> Within the former, carbon-carbon bonds are notably alternated, going from 1.380Å and 1.376Å for *rim*- and *spoke*-bonds to 1.438Å and 1.409Å for *flank*- and *hub*-ones. In the most stable isomer among functionalized cations, [CH<sub>3</sub>-*hub*-C<sub>20</sub>H<sub>10</sub>]<sup>+</sup>, the situation with *rim*- and *spoke*-C-C bonds remains essentially the same as in neutral corannulene (Table 1), with only one exception, namely, the C1-C2 bond of attachment, which shows significant elongation (1.477Å vs. 1.377Å-1.392Å for other *spoke*-bonds). In contrast, C-C bonds in central five-membered ring undergo significant perturbations. In unperturbed C<sub>20</sub>H<sub>10</sub> these bonds are all equal to 1.409Å. In [CH<sub>3</sub>-*hub*-C<sub>20</sub>H<sub>10</sub>]<sup>+</sup>, two bonds are shortened down to 1.377Å, one bond is slightly longer (1.420Å), and two other

bonds are dramatically elongated (1.481Å). Such changes make this ring structurally close to what was observed for cyclopentadiene molecule (Table 1).

In other two isomers, *rim*- and *spoke*-ones, the central ring shows relatively small changes during functionalization in comparison with neutral C<sub>20</sub>H<sub>10</sub> (the largest deviation Δ=0.08Å and 0.02Å, respectively). Functionalization of corannulene bowl at *spoke* site revealed dramatic elongation of two of ten *flank* bonds (C2-C3 in Table 1), while the others show no significant changes. Similar, binding of CH<sub>3</sub><sup>+</sup> group to the *rim* site led to elongation of both C2-C3 and C3-C4 bonds.

Altogether, these findings indicate that adding methyl cation to any carbon atom of the bowl moiety results in dramatic elongation of all C-C bonds, surrounding site of attachment. Such increase of bond length is in agreement with their transformation from multiple carbon-carbon bonds to single bond of σ-type, observed previously. This conclusion is well-supported by calculation of Wiberg bond orders (Table 1).

Formation of a sequence of single C-C bonds should break π-delocalization. However, in the case of *hub*-isomer, such breaking is expected mainly for the central 5-membered ring and only slightly for the system of *rim*- and *flank*-bonds. Calculation of structure-related descriptor HOMA for all rings in bowl-shaped fragment clearly supported this statement (Table 2). This index is equal to 1.00 for benzene molecule, in which delocalization is considered to be ideal. For rings A2 and A3 the delocalization stays the same as in neutral corannulene or becomes even stronger, whereas for the ring B delocalization is completely vanished. Significant decrease of delocalization was also found for rings A1, which can be attributed to the formation of single σ-bond (C1-C2) instead of original double bond.

**Table 2.** Aromaticity indexes calculated for functionalized corannulene cations as well as for the group of selected reference molecules (PBE0/cc-pVTZ).

System		HOMA <sup>a</sup>	NICS	AIM <sup>b</sup>		Fuzzy Atomic Space <sup>c</sup>	
				PDI	FLU	PDI	FLU
C <sub>6</sub> H <sub>6</sub>		1.000	-8.21	0.105	0.000	0.106	0.000
C <sub>5</sub> H <sub>5</sub> <sup>-</sup>		0.907	-14.31		0.000		0.000
C <sub>5</sub> H <sub>6</sub>		-0.622	-3.43		0.054		0.043
C <sub>20</sub> H <sub>10</sub>	A	0.702	-6.43	0.059	0.014	0.060	0.019
	B	0.818	9.22		0.026		0.038
[R- <i>hub</i> -C <sub>20</sub> H <sub>10</sub> ] <sup>+</sup>	A1	0.198	-7.61	0.033	0.035	0.037	0.042
	A2	0.799	-6.40	0.057	0.012	0.059	0.017
	A3	0.854	-12.86	0.048	0.014	0.050	0.021
	B	0.045	-3.26		0.047		0.060
[R- <i>rim</i> -C <sub>20</sub> H <sub>10</sub> ] <sup>+</sup>	A1	-0.228	-0.64	0.026	0.035	0.031	0.038
	A2	0.787	-1.28	0.062	0.011	0.064	0.016
	A3	0.746	-6.52	0.061	0.014	0.062	0.020
	A4	0.776	0.28	0.053	0.014	0.056	0.020
	A5	0.623	-1.74	0.042	0.022	0.045	0.028
	B	0.892	13.70		0.027		0.038
[R- <i>spoke</i> -C <sub>20</sub> H <sub>10</sub> ] <sup>+</sup>	A1	-0.024	0.53	0.032	0.043	0.036	0.050
	A2	0.772	2.27	0.054	0.014	0.056	0.020
	A3	0.790	-7.76	0.063	0.013	0.065	0.018
	B	0.890	13.61		0.025		0.036

<sup>a</sup> Reference for C-C bond length in HOMA is 1.388 Å and  $\alpha=257.7$  as obtained from geometry of benzene molecule optimized at the same level of theory. <sup>b</sup> Atomic overlap matrix is based on basin integral in the Bader's AIM.<sup>32</sup> <sup>c</sup> Atomic overlap matrix is based on fuzzy atom space integral over the Becke atomic space.<sup>33</sup> Reference delocalization index for C-C bond for the Bader's FLU is equal to 1.3921e as taken from benzene, whereas in the Becke's variant of FLU, it is equal to 1.4637e

In  $[\text{CH}_3\text{-rim-C}_{20}\text{H}_{10}]^+$  system, delocalization in ring B remains untouched, whereas 6-membered rings undergo dramatic transformations. It is mostly pronounced for ring A1, for which HOMA index changes from 0.818 in neutral  $\text{C}_{20}\text{H}_{10}$  to -0.228 in target cationic species. Delocalization in rings A2, A3, and A4 stays unchanged, while in ring A6 it is slightly decreased (Table 2). Similar situation was observed for the *spoke*-isomer, in which two symmetry equivalent rings A1 show complete loss of delocalization, whereas rings A2 and A3 show essentially the same delocalization as in unperturbed corannulene. Ring B also remains unchanged and shows strong delocalization.

## II. $\pi$ -Delocalization

Next, we turned to considering  $\pi$ -delocalization indexes based on topological quantum theory within the framework of Bader's Atom In Molecule theory.<sup>31</sup> Selected indexes are *para*-DI (or PDI) and FLU (in two alternative variants). Calculated values for both descriptors are collected in Table 2. Importantly, PDI can only be applied to 6-membered rings. At the same time, FLU descriptor can be applied to ring of any dimension. For comparison, the same indexes were calculated, when possible, for small model systems such as benzene, cyclopentadienyl anion and cyclopentadiene (Table 2).

Calculated PDI and FLU parameters are in good agreement with previously discussed HOMA indexes. PDI index for ring A in neutral  $\text{C}_{20}\text{H}_{10}$  expectedly showed twice smaller delocalization than that in benzene. Subsequent functionalization of corannulene bowl by methylation at hub site resulted in further decrease of delocalization of  $\pi$ -electrons for rings A1 and A3, whereas for ring A2 it remained almost unchanged (Table 2). The same trend was observed

for both types of PDI, proposed by Bader<sup>32</sup> and by Becke.<sup>33</sup> FLU indexes, which are actually measuring the relative electronic divergences of a given ring in a molecule of interest relative to a molecule chosen as a reference (here – benzene). So, the smaller the FLU index is, the closer the delocalization in considered ring to that in C<sub>6</sub>H<sub>6</sub>. In other words, smaller FLU values indicate stronger delocalization (for C<sub>6</sub>H<sub>6</sub> FLU=0.000). In accordance with this, delocalization in ring A of C<sub>20</sub>H<sub>10</sub> is notably smaller than that in reference molecule. At the same time, delocalization in the case of ring B was found even smaller albeit not dramatically. Formation of [CH<sub>3</sub>-*hub*-C<sub>20</sub>H<sub>10</sub>]<sup>+</sup> expectedly showed significant reducing of delocalization in rings A1 and B, whereas changes in delocalization in rings A2 and A3 are only tiny as compared with unperturbed neutral corannulene (Table 2).

Both PDI and FLU indexes consistently revealed significant reduce of delocalization in ring A1 in [CH<sub>3</sub>-*rim*-C<sub>20</sub>H<sub>10</sub>]<sup>+</sup>, whereas rings A2 and A3 show some increase of delocalization in comparison with C<sub>20</sub>H<sub>10</sub> (Table 2). Notable decrease of delocalization was also observed for ring A5. Ring A4 was found to be unchanged. Interestingly, FLU parameter calculated for ring B indicated strong delocalization of  $\pi$ -electrons, comparable with those in neutral corannulene. Similar results were obtained for [CH<sub>3</sub>-*spoke*-C<sub>20</sub>H<sub>10</sub>]<sup>+</sup> system, in which the central 5-membered ring B shows almost no changes when going from neutral to cationic species. Ring A1 shows notable decrease of delocalization, whereas for ring A3 the opposite trend was observed. Ring A2 does not undergo any significant changes in  $\pi$ -delocalization (Table 2).

Correlation between aforementioned HOMA parameters and PDI and FLU indexes was found to be excellent for all cationic systems considered in this study (Table 2).

### III. Magnetic Aspects

Magnetic aspects of aromaticity includes many different topics such as (but not limited by) magnetic susceptibility, the exaltation,<sup>40</sup> anisotropy of magnetic susceptibility,<sup>41</sup> nucleus independent chemical shift (NICS<sup>26</sup>) and others. In this study, we used a set of methods/techniques to analyze changes in aromaticity in target cationic species, which includes: (i) anisotropy of the induced current density (ACID) approach,<sup>36</sup> (ii) NICS,<sup>26</sup> calculated at the center of the ring(s), and (iii) chemical shift, calculated for all hydrogen and carbon atoms (with respect to tetramethylsilane, TMS).

#### III.1. ACID approach

The current density, which indicates ring currents in aromatic systems, comes closer to a more general definition of delocalization. The current density is a vector field with vectors assigned to each point of space. The length of the vectors is proportional to the magnitude of the current. The power of ring current mapping as tool for visualizing and understanding aromaticity was proven.<sup>42</sup> However, in systems without cyclic conjugation such linear or branched polyenes or in non-planar systems the topology of the currents can be extremely complicated and thus difficult to interpret. In analogy with anisotropy of the magnetic susceptibility, the anisotropy of the current (induced) density was introduced by Geuenuch *et al.*<sup>36,43</sup> ACID is exclusively a function of the paramagnetic part of the current density, which is determined by the perturbation of the wavefunction by the magnetic field. Importantly, the ACID function represents mainly anisotropies of interatomic current and, thus, the delocalized electrons, and being 3D-function can be applied to systems of any topology. In this study, the ACID functions were calculated for

all cationic species under consideration as well as for neutral corannulene for the sake of comparison.

Current density vectors plotted onto the ACID surface calculated for unperturbed  $C_{20}H_{10}$  (Fig. 2) unambiguously revealed the presence of very strong diatropic current, which goes over all *rim-* and *flank-*bonds. This can be attributed to pronounced aromatic behavior of all 6-membered rings in corannulene. At the same time, the central 5-membered ring shows significant paratropic current, which indicates its anti-aromatic behavior. Subsequent subtraction of  $\pi$ -component (Fig. 3) revealed the key role of  $\pi$ -delocalization in total electron delocalization in  $C_{20}H_{10}$  molecule. This combination of aromatic exterior part and anti-aromatic interior part in corannulene was previously discussed in detail.<sup>7,31,39</sup>

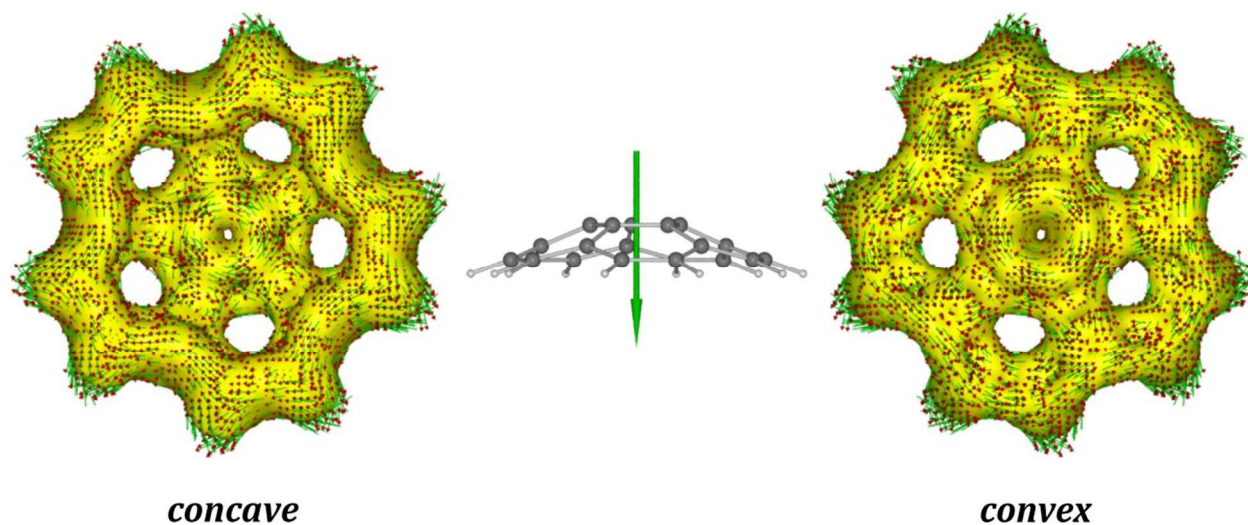


**Figure 2.** ACID isosurfaces of neutral corannulene. Current density vectors are plotted onto the ACID isosurface to indicate dia- and paratropic ring currents. Green arrow in the middle ball-and-stick model shows applied magnetic field direction.

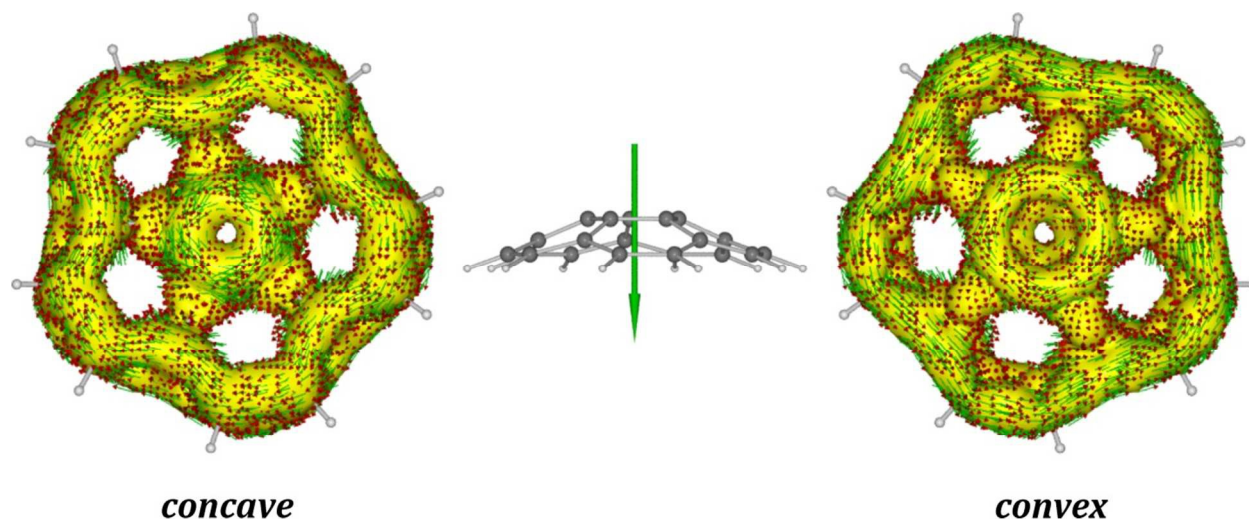


**Figure 3.**  $\pi$ -Contribution to the ACID isosurface of neutral corannulene. Current density vectors are plotted onto the ACID isosurface to indicate dia- and paratropic ring currents. Green arrow in the middle ball-and-stick model shows applied magnetic field direction.

Functionalization of corannulene moiety at the *rim*-site with methyl cation leads to significant perturbations in anti-aromatic behavior of the central 5-membered ring (Fig. 4). In  $[\text{CH}_3\text{-hub-C}_{20}\text{H}_{10}]^+$  this ring B is not anti-aromatic anymore. It shows behavior similar with those of cyclopentadiene. On the other hand, the aromatic delocalization that goes over all *rim*- and *flank*-bonds remains almost untouched and shows high similarity with that in unperturbed corannulene (Fig. 2). These findings become even more pronounced when considering  $\pi$ -contribution (Fig. 5). This is in full agreement with previous conclusions based on structural and topological descriptors. Thus, functionalization at the interior sites (*hub*) results in vanishing destabilizing anti-aromatic character of the central five-membered ring (transforming it to slightly aromatic cyclopentadiene-like ring), whereas keeping stabilizing aromatic behavior of 6-membered rings alive.

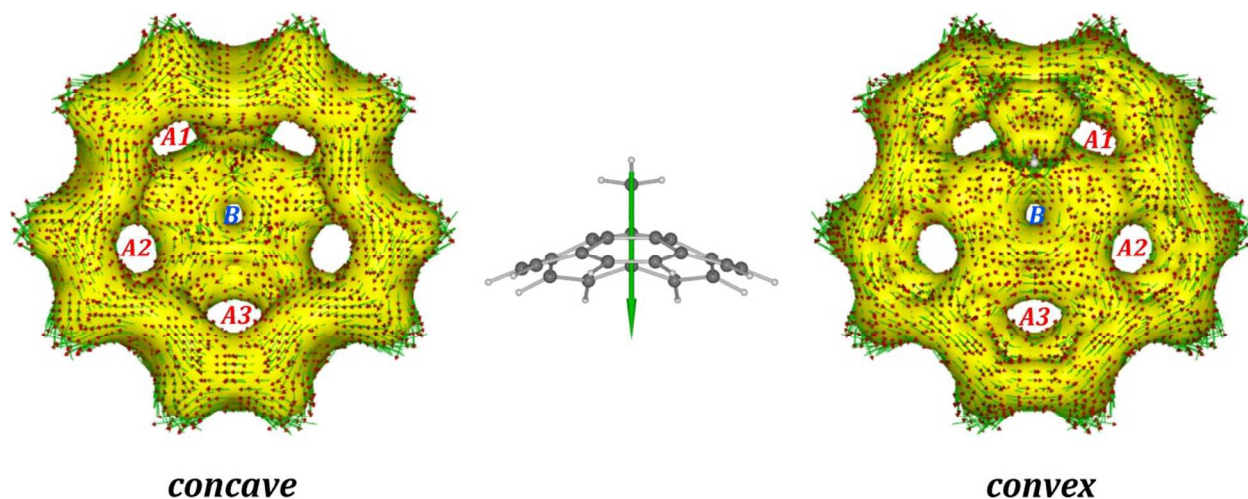


**Figure 4.** ACID isosurfaces of cationic  $[\text{CH}_3\text{-hub-C}_{20}\text{H}_{10}]^+$ . Current density vectors are plotted onto the ACID isosurface to indicate dia- and paratropic ring currents. Green arrow in the middle ball-and-stick model shows applied magnetic field direction.

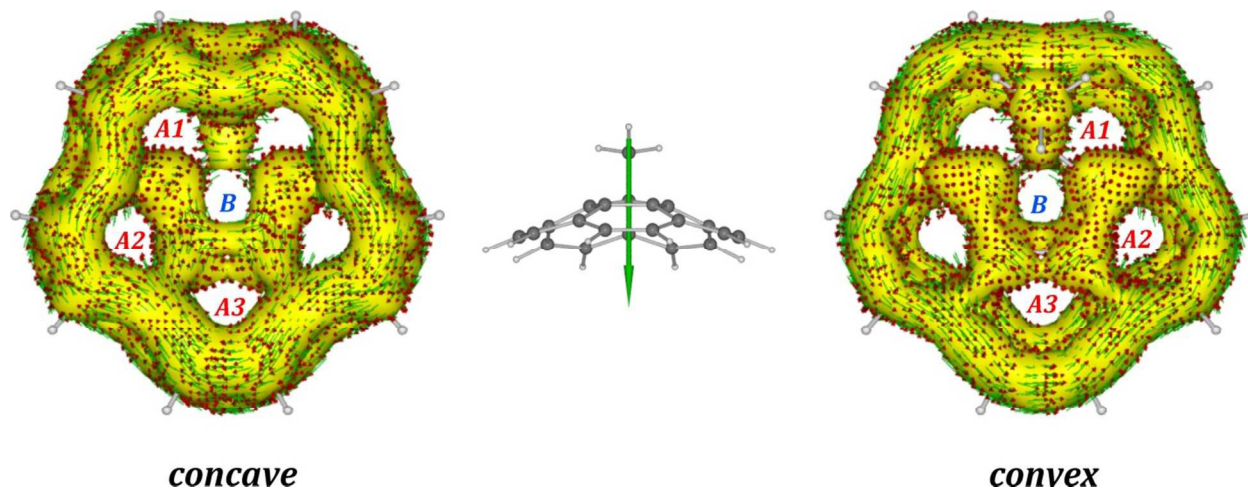


**Figure 5.**  $\pi$ -Contribution to the ACID isosurface of cationic  $\{\text{CH}_3\text{-hub-C}_{20}\text{H}_{10}\}^+$ . Current density vectors are plotted onto the ACID isosurface to indicate dia- and paratropic ring currents. Green arrow in the middle ball-and-stick model shows applied magnetic field direction.

In contrast, functionalization of the corannulene bowl at *rim*- and *spoke*-sites completely disrupts the stabilizing aromatic delocalization over *rim*- and *flank*-bonds. It is especially pronounced for  $\pi$ -delocalization (Fig. 6 and Fig. 7). At the same time, strong paratropic current was found in central ring for both isomers. It means that destabilizing anti-aromatic behavior of ring B in the bowl still exists and works against stability of these functionalized cations.

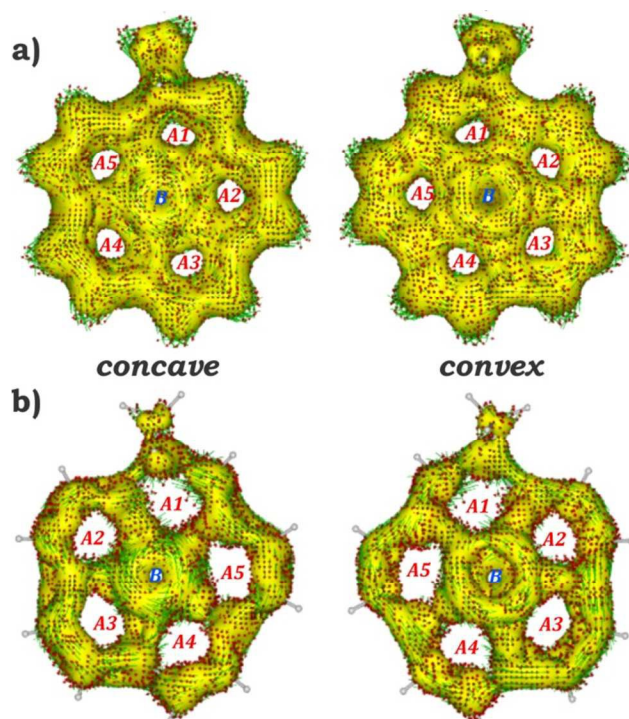


**Figure 6.** ACID isosurfaces of cationic  $[\text{CH}_3\text{-rim-C}_{20}\text{H}_{10}]^+$  (a) and its  $\pi$ -contribution (b). Current density vectors are plotted onto the ACID isosurface to indicate dia- and paratropic ring currents. The magnetic field vector is orthogonal with respect to 5-membered ring plane and directed downward (in the same way as it is in neutral corannulene and *hub*-isomer).

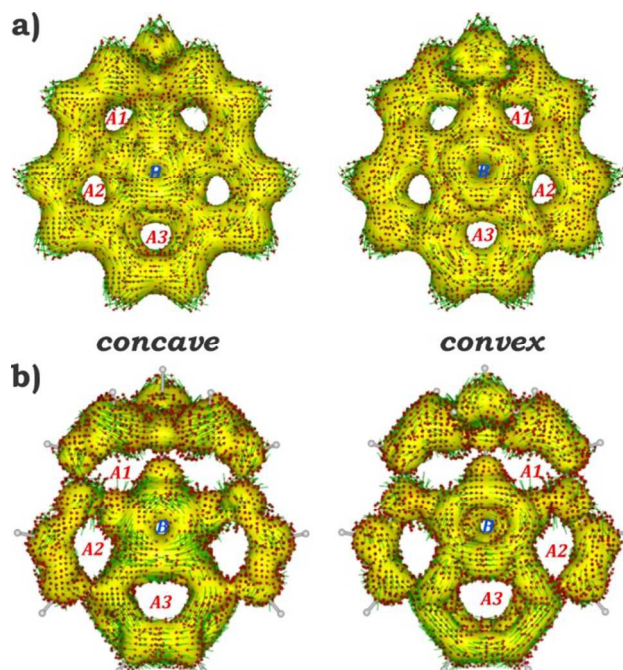


**Figure 7.** ACID isosurfaces of cationic  $[\text{CH}_3\text{-spoke-C}_{20}\text{H}_{10}]^+$  (a) and its  $\pi$ -contribution (b). Current density vectors are plotted onto the ACID isosurface to indicate dia- and paratropic ring currents. The magnetic field vector is orthogonal with respect to 5-membered ring plane and directed downward (in the same way as it is in neutral corannulene and *hub*-isomer).

### III.2. NICS

Next, the nucleus independent chemical shift (NICS) was calculated in order to get further insights into the aromaticity in target cationic species and changes it experiences when going from unperturbed corannulene to  $[\text{CH}_3\text{-C}_{20}\text{H}_{10}]^+$  systems. In this study we used NICS(0), which is calculated at the center of the ring under consideration. Previously, it was shown that NICS(1), calculated in  $1\text{\AA}$  above the surface provides more pronounced picture of  $\pi$ -delocalization in planar polyaromatic molecules. However, in the case of curved PAHs, NICS(1) will give two

different value for convex and concave surfaces. Thus, NICS(0) seems to be more balanced descriptor (hereafter NICS). Results of NICS calculations for all systems considered are summarized in Table 2.

Calculated NICS values for rings A and B in neutral corannulene revealed their clear aromatic (-6.43 ppm) and anti-aromatic (+9.22 ppm) behavior, respectively (Table 2). These findings are in full agreement with previously published results and with results based on HOMA, PDI, FLU and ACID descriptors, calculated in this study. Subsequent functionalization of corannulene bowl by methyl cation at *hub*-site resulted in removing an anti-aromatic character of the center 5-membered ring, whereas all 6-membered rings show pronounced aromatic behavior. At the same time, attachment of  $\text{CH}_3^+$  group to *rim*- or *spoke*-carbon atom led to opposite results – central ring remained anti-aromatic in nature, while the aromaticity of rings A1, A2, A4, and A5 in  $[\text{CH}_3\text{-rim-C}_{20}\text{H}_{10}]^+$  and rings A1 and A2 in  $[\text{CH}_3\text{-spoke-C}_{20}\text{H}_{10}]^+$  completely vanished. Significant aromaticity was observed only for rings A3 in both isomers.

### III.3. Chemical shifts

At the final step in our investigation, chemical shifts for hydrogen ( $^1\text{H-NMR}$ ) and carbon ( $^{13}\text{C-NMR}$ ) atoms were calculated. All numbers were computed using TMS as the reference compound, optimized at the same level of theory.

*Hub*-functionalized cation  $[\text{CH}_3\text{-hub-C}_{20}\text{H}_{10}]^+$  shows two groups of peaks in calculated  $^1\text{H NMR}$  spectrum (Fig. 8), which correspond to aliphatic  $\text{CH}_3$ -group in the range -0.2 – 0.00 ppm and to resonance signals of the aromatic protons in the range from 9.0 ppm to 9.5 ppm. These data agree with previously reported experimental values,<sup>16</sup> thus providing additional proof for reliability of computed results and selected level of theory. Interestingly, attachment of  $\text{CH}_3$ -

cation to the *hub*-carbon atom showed no dramatic changes in resonance signals of aromatic protons. For instance, value of 8.2 ppm was calculated for unperturbed corannulene (see Supporting Information for details), showing that aromatic delocalization that goes over all *rim*- and *flank*-bonds stays undestroyed during *hub*-functionalization. It is in full agreement with previous conclusions, which were based on different descriptors of aromaticity. Essentially the same situation was observed in  $^{13}\text{C}$  NMR shifts for *rim*-carbon atoms (135.9-139.7 ppm vs. 132.1 ppm in  $\text{C}_{20}\text{H}_{10}$ ), except for C4 ( $\delta=155.6$  ppm), which is in *para*-position with respect to the carbon atom of attachment. The most pronounced effect of functionalization was found in the case of *hub*-carbon atoms of the central ring. The C1 atom shows resonance signal at 56.9 ppm, thus, confirming its transformation from aromatic (145.8 ppm in  $\text{C}_{20}\text{H}_{10}$ ) to aliphatic carbon atom. Its neighboring C6 atoms show signal at 175.6 ppm.  $^{13}\text{C}$  calculated chemical shifts are also in very good agreement with previously observed experimental ones.<sup>16</sup>

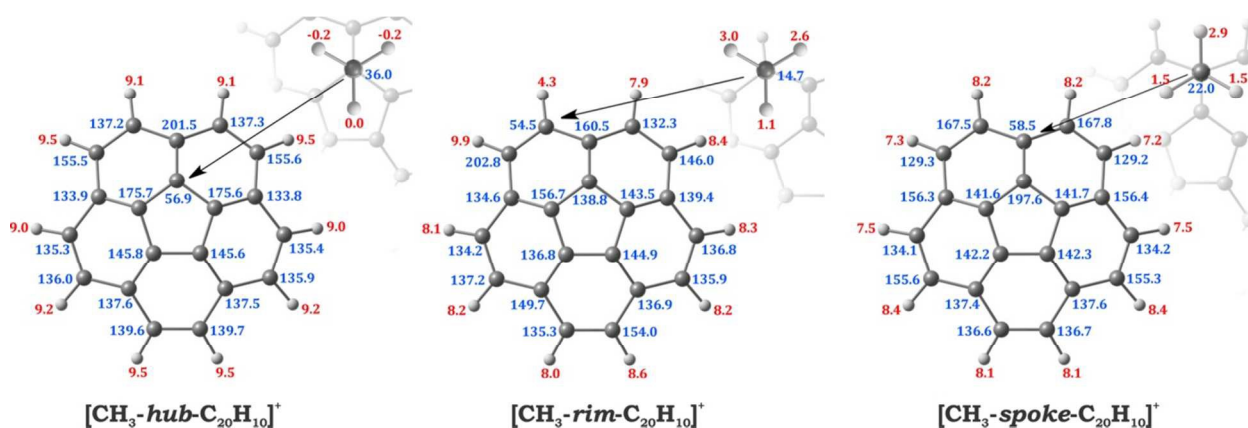


**Figure 8.** Calculated  $^1\text{H}$  and  $^{13}\text{C}$  NMR chemical shifts in different isomers of functionalized corannulene cations. Black arrows point the carbon atom of attachment.

$[\text{CH}_3\text{-rim-C}_{20}\text{H}_{10}]^+$  and  $[\text{CH}_3\text{-spoke-C}_{20}\text{H}_{10}]^+$  show much wider range for proton resonance signals from 4.3 ppm to 9.9 ppm and from 7.2 ppm to 8.4 ppm (Fig. 8), respectively. This finding clearly indicates significant perturbations in aromatic systems of 6-membered rings during functionalization. Similar,  $^{13}\text{C}$  NMR signals for *rim* atoms also show wide range of values from 132.3 ppm to 202.8 ppm for *rim*-isomer and from 129.2 ppm to 167.8 ppm for *spoke*-functionalized cation. Importantly, in both isomers *rim* and *spoke* the atom of attachment undergoes transformation from being aromatic in unperturbed corannulene to aliphatic in cationic species (with signals of 54.5 ppm and 58.5 ppm, respectively). The same situation was observed in *hub*-isomer (Fig. 8), but with different consequences. Making one of *rim*- or *flank*-carbon atom aliphatic dramatically disrupts delocalization over the exterior part of corannulene bowl and, as consequence, destroys its aromatic system. At the same time, *hub*-carbon atoms in  $[\text{CH}_3\text{-rim-C}_{20}\text{H}_{10}]^+$  and  $[\text{CH}_3\text{-spoke-C}_{20}\text{H}_{10}]^+$  isomers stay aromatic (corresponding resonance signals are from 136.8 ppm to 156.7 ppm and from 141.7 ppm to 197.6 ppm).

## Concluding remarks

In this study, the first comprehensive theoretical investigation of aromaticity in functionalized corannulene cations of general formula  $[\text{CH}_3\text{-C}_{20}\text{H}_{10}]^+$  was accomplished. The experimentally known system  $[\text{CH}_3\text{-hub-C}_{20}\text{H}_{10}]^+$  was augmented by two other possible isomers, namely, *rim*- and *spoke*-ones. In order to get most completed picture of aromaticity in target systems, a set of aromaticity descriptors of different nature was used. This set included structure-based HOMA, topological descriptors PDI and FLU (in two variants, proposed by Bader<sup>32</sup> and Becke<sup>33</sup>), and magnetic NICS. Highly efficient tool for analysis and visualization of delocalization and conjugation named ACID was also utilized. Additionally, a complete set of  $^1\text{H}$  and  $^{13}\text{C}$  chemical shifts was calculated. Results were compared with those for reference molecules such as unperturbed neutral corannulene, benzene, cyclopentadiene, and cyclopentadienyl anion.

In spite of being different in terms of theory, all descriptors showed very good correlation. It was found that attaching the methyl cation to any of carbon atom of the curved polyaromatic bowl of corannulene results in disruption of delocalization in neighboring rings. However, consequences of this disruption are dramatically different for different isomers of  $[\text{CH}_3\text{-C}_{20}\text{H}_{10}]^+$ . For instance, in the case of *hub*-isomer, attaching  $\text{CH}_3^+$  group to the bowl led to crashing of delocalization in central 5-membered ring, which is anti-aromatic in nature. Removal of destabilizing anti-aromatic part expectedly resulted in increase of stability of the target functionalized cationic species. On the other hand, delocalization over *rim*- and *flank*-bonds remained only slightly influenced and thus all 6-membered rings still show strong stabilizing aromatic behavior.

In contrast, adding methyl cation to *rim* or *spoke* carbon atom led to opposite situation when stabilizing aromatic character of neighboring 6-membered rings vanished, whereas anti-aromatic behavior of the central 5-membered ring stayed almost unchanged. As consequences, stability of these cationic species was found to be low in comparison with that of *hub*-isomer.

Altogether, it provides a pretty solid explanation of high stability of *hub*-isomer and reliable interpretation of previous experimental results,<sup>16</sup> which showed an absence of any traces of other isomers.

## ASSOCIATED CONTENT

### Supporting Information

Computational details; Coordinates and energies of all calculated model adducts; NBO charges and Wiberg bond orders for all atoms in the calculated complexes.

## AUTHOR INFORMATION

### Corresponding Author

[andrey.rogachev@iit.edu](mailto:andrey.rogachev@iit.edu) and/or [andrey.rogachev@gmail.com](mailto:andrey.rogachev@gmail.com)

### Notes

The authors declare no competing financial interest.

## ACKNOWLEDGEMENTS

Financial support from Illinois Institute of Technology (start-up funds, A.Yu.R) is greatly acknowledged. We also thank Dr. A. A. Granovsky and Firefly team for providing the developing version of the Firefly program and numerous helpful discussions.

## References

- <sup>1</sup> H. W. Kroto, J. R. Heath, S. C. O'Brien, R. F. Curl, R. E. Smalley, *Nature*, 1985, **318**, 162.
- <sup>2</sup> J. R. Heath, S. C. O'Brien, Q. Zhang, Y. Liu, R. F. Tittel, R. E. Smalley, *J. Am. Chem. Soc.*, 1985, **107**, 7779.
- <sup>3</sup> S. Iijima, *Nature*, 1991, **354**, 56.
- <sup>4</sup> (a) M. S. Dresselhaus, G. Dresselhaus, J. C. Charlier, E. Hernández, *Phil. Trans. R. Lond. A*, 2004, **362**, 2065. (b) S. B. Sinnott, R. Andrews, *Crit. Rev. Solid State*, 2001, **26**, 145.
- <sup>5</sup> T. Dürkop, S. A. Getty, E. Cobas, M. S. Fuhrer, *Nano Lett.*, 2004, **4**, 35.
- <sup>6</sup> K. S. Novoselov, A. K. Geim, S. V. Mironov, D. Jiang, Y. Zhang, S. V. Dubonos, I. V. Grigorieva, A. A. Forsi, *Science*, 2004, **306**, 666.
- <sup>7</sup> *Fragments of Fullerenes and Carbon Nanotubes*, Ed. M.A. Petrukhina, L.T. Scott, John Wiley & Sons, Inc. Hoboken, New Jersey, **2012**.
- <sup>8</sup> (a) T. Amaya, T. Hirao, *Chem. Commun.*, 2011, **47**, 10524. (b) S. Higashibayashi, H. Sakurai, *Chem. Lett.*, 2011, **40**, 122. (c) A. Sygula, *Eur. J. Org. Chem.*, 2011, 1611. (d) Y. - T. Wu, J. S. Siegel, *Chem. Rev.*, 2006, **106**, 4843. (e) V. M. Tsefricas, L.T. Scott, *Chem. Rev.*, 2006, **106**, 4868. (f) P. W. Rabideau, A. Sygula, *Acc. Chem. Res.*, 1996, **29**, 235.
- <sup>9</sup> (a) E. A. Jackson, B. D. Steinberg, M. Bancu, A. Wakamiya, L. T. Scott, *J. Am. Chem. Soc.*, 2007, **129**, 484. (b) B. D. Steinberg, E. A. Jackson, A. S. Filatov, A. Wakamiya, M. A. Petrukhina, L. T. Scott, *J. Am. Chem. Soc.*, 2009, **131**, 10537. (c) A. S. Filatov, L. T. Scott, M. A. Petrukhina, *Cryst. Growth Design*, 2010, **10**, 4607. (d) T. - C. Wu, H. - J. Hsin, M. - Y. Kuo, C - H. Li, Y. - T. Wu, *J. Am. Chem. Soc.*, 2011, **133**, 16319.
- <sup>10</sup> A. Sygula, W.E. Collier, "Molecular Clips and Tweezers with Corannulene Pincers", in *Fragments of Fullerenes and Carbon Nanotubes*, Ed. M.A. Petrukhina, L.T. Scott, John Wiley & Sons, Inc. Hoboken, New Jersey, **2012**, p.1-41.
- <sup>11</sup> See for instance: (a) J.B. Goodenough, K.-S. Park, *J. Am. Chem. Soc.*, 2013, **135**, 1167. (b) L.L. Zhang, X.S. Zhao, *Chem. Soc. Rev.*, **2009**, **38**, 2520. (c) J. Chen, C. Li, G. Shi, *J. Phys. Chem. Lett.*, 2013, **4**, 1244.
- <sup>12</sup> (a) Y.-T. Wu, D. Bandera, R. Maag, A. Linden, K. K. Baldrige, J. S. Siegel, *J. Am. Chem. Soc.*, 2008, **130**, 10729. (b) K. K. Baldrige, K. I. Hardcastle, T. J. Seiders, J. S. Siegel, *Org. Biomol. Chem.*, 2010, **8**, 53. (c) Q. Zhang, K. Kawasumi, Y. Segawa, K. Itami, L. T. Scott, *J. Am. Chem. Soc.*, 2012, **134**, 15664. (d) M. Mattarella, J. S. Siegel, *Org. Biomol. Chem.*, 2012, **10**, 5799. (e) B. M. Schmidt, B. Topolinski, P. Roesch, D. Lentz, *Chem. Commun.*, 2012, **48**, 6520. (f) Y.-L. Wu, M. C. Stuparu, C. Boudon, J.-P. Gisselbrecht, W. B. Schweizer, K. K. Baldrige, J. S. Siegel, F. Diederich, *J. Org. Chem.*, 2012, **77**, 11014. (g) D. Eisenberg, J. M. Quimby, D. Ho, R. Lavi, L. Benisvy, L. T. Scott, R. Shenhar, *Eur. J. Org. Chem.*, 2012, 6321. (h) A. K. Greene, L. T. Scott, *J. Org.*

*Chem.*, 2013, **78**, 2139. (i) M. Yamada, S. Tashiro, R. Miyake, M. Shionoya, *Dalton Trans.*, 2013, **42**, 3300. (j) M. Mattarella, L. Berstis, K. K. Baldrige, J. S. Siegel, *Bioconjugate Chem.*, 2014, **25**, 115. (k) B. Topolinski, B. M. Schmidt, S. Schwagerus, M. Kathan, D. Lentz, *Eur. J. Inorg. Chem.*, 2014, 5391. (l) J. Kang, D. Miyajima, Y. Itoh, T. Mori, H. Tanaka, M. Yamauchi, Y. Inoue, S. Harada, T. Aida, *J. Am. Chem. Soc.*, 2014, **136**, 10640.

<sup>13</sup> (a) M. Mattarella, J. M. Haberl, J. Ruokolainen, E. M. Landau, R. Mezzenga, J. S. Siegel, *Chem. Commun.* **2013**, 49, 7204. (b) D. Miyajima, K. Tashiro, F. Araoka, H. Takezoe, J. Kim, K. Kato, M. Takata, T. Aida, *J. Am. Chem. Soc.* **2009**, *131*, 44.

<sup>14</sup> (a) I. V. Kuvychko, S. N. Spisak, Y.-S. Chen, A. A. Popov, M. A. Petrukhina, S. H. Strauss, O. V. Boltalina, *Angew. Chem. Int. Ed.*, 2012, **51**, 4939. (b) B. M. Schmidt, S. Seki, B. Topolinski, K. Ohkubo, S. Fukuzimi, H. Sakurai, D. Lentz, *Angew. Chem. Int. Ed.*, 2012, **51**, 11385. (c) I. V. Kuvychko, C. Dubceac, S. H. M. Deng, X.-B. Wang, A. A. Granovsky, A. A. Popov, M. A. Petrukhina, S. H. Strauss, O. V. Boltalina, *Angew. Chem. Int. Ed.*, 2013, **52**, 7505. (d) B. M. Schmidt, B. Topolinski, M. Yamada, S. Higashibayashi, M. Shionoya, H. Sakurai, D. Lentz, *Chem. Eur. J.*, 2013, **19**, 13872.

<sup>15</sup> V. Boekelheide, *Pure Appl. Chem.*, 1975, **44**, 751.

<sup>16</sup> (a) A. V. Zabula, S. N. Spisak, A. S. Filatov, A. Yu. Rogachev, M. A. Petrukhina, *Angew. Chem.*, 2011, **123**, 3027; *Angew. Chem. Int. Ed.*, 2011, **50**, 2971. (b) C. Dubceac, A. V. Zabula, A. S. Filatov, F. Rossi, P. Zanello, M. A. Petrukhina, *J. Phys. Org. Chem.*, 2012, **25**, 553. (c) C. Dubceac, A. S. Filatov, A. V. Zabula, A. Yu. Rogachev, M. A. Petrukhina, *Chem. Eur. J.*, 2015, **21**, 14268. (d) A. V. Zabula, C. Dubceac, A. S. Filatov, M. A. Petrukhina, *J. Org. Chem.*, 2011, **76**, 9572.

<sup>17</sup> A. Yu. Rogachev, A. S. Filatov, A. V. Zabula, M. A. Petrukhina, *Phys. Chem. Chem. Phys.*, 2012, **14**, 3554.

<sup>18</sup> (a) T. Kitagawa, H. Sakamoto, K. Takeuchi, *J. Am. Chem. Soc.*, 1999, **121**, 4298. (b) T. Kitagawa, Y. Lee, N. Masaoka, K. Komatsu, *Angew. Chem. Int. Ed.*, 2005, **44**, 1398. (c) T. Kitagawa, in *Recent Developments in Carbocation and Onium Ion Chemistry*, ed. K. Laali, ACS Symposium Series; American Chemical Society: Washington, DC, 2007. (d) Y. Murata, F. Cheng, T. Kitagawa, K. Komatsu, *J. Am. Chem. Soc.*, 2004, **126**, 8874. (e) C. A. Reed, K.-C. Kim, R. D. Bolskar, L. J. Muller, *Science*, 2000, **289**, 101. (f) L. J. Muller, D. W. Elliot, K.-C. Kim, C. A. Reed, P. D. W. Boyd, *J. Am. Chem. Soc.*, 2002, **124**, 9360.

<sup>19</sup> L. T. Scott, H. E. Bronstein, D. V. Preda, R. B. M. Ansems, M. S. Bratcher and S. Hagen, *Pure Appl. Chem.*, 1999, **71**, 209.

<sup>20</sup>(a) J. P. Perdew, K. Burke, M. Ernzerhof, *Phys. Rev. Lett.*, 1997, **78**, 1396. (b) J. P. Perdew, K. Burke, M. Ernzerhof, *Phys. Rev. Lett.*, 1996, **77**, 3865.

<sup>21</sup> A. A. Granovsky, *Firefly version 8.1.0*, www <http://classic.chem.msu.su/gran/firefly/index.html>

- 
- <sup>22</sup> (a) F. Weinhold, C. A. Landis, *Valency and Bonding: A Natural Bond Orbital Donor – Acceptor Perspective*. Cambridge University Press: Cambridge, 2005. (b) A. E. Reed, L. A. Curtiss, F. Weinhold, *Chem. Rev.*, 1988, **88**, 899.
- <sup>23</sup> K. Wiberg, *Tetrahedron*, 1968, **24**, 1083.
- <sup>24</sup> (a) E. D. Glendening, J. K. Badenhop, A. E. Reed, J. E. Carpenter, J. A. Bohmann, C. M. Morales, F. Weinhold, *NBO 6.0*, **2013**, University of Wisconsin, Madison. (b) E. D. Glendening, C. R. Landis, F. Weinhold, *J. Comp. Chem.*, 2013, **34**, 1429.
- <sup>25</sup> (a) J. Kruszewski, T. M. Krygowski, *Tetrahedron Lett.*, 1972, **13**, 3839. (b) T. M. Krygowski, *J. Chem. Inf. Comp. Sci.*, 1993, **33**, 70.
- <sup>26</sup> (a) P. von Ragué Schleyer, C. Maerker, A. Dransfeld, H. Jiao, N. J. R. van EikemaHommes, *J. Am. Chem. Soc.*, 1996, **118**, 6317. (b) Z. Chen, C. S. Wannere, C. Corminboeuf, R. Puchta, P. von Ragué Schleyer, *Chem. Rev.*, 2005, **105**, 3842.
- <sup>27</sup> (a) P. Lazzeretti, *Phys. Chem. Chem. Phys.*, 2004, **6**, 217. (b) S. Fias, S. van Damme, P. Bultinck, *J. Comput. Chem.*, 2008, **29**, 358. (c) I. V. Omelchenko, O. V. Shishkin, L. Gorb, J. Leszczynsky, S. Fias, P. Bultinck, *Phys. Chem. Chem. Phys.*, 2011, **13**, 20536.
- <sup>28</sup> *Gaussian 09, Revision D.01*, M. J. Frisch, G. W. Trucks, H. B. Schlegel, G. E. Scuseria, M. A. Robb, J. R. Cheeseman, G. Scalmani, V. Barone, B. Mennucci, G. A. Petersson, H. Nakatsuji, M. Caricato, X. Li, H. P. Hratchian, A. F. Izmaylov, J. Bloino, G. Zheng, J. L. Sonnenberg, M. Hada, M. Ehara, K. Toyota, R. Fukuda, J. Hasegawa, M. Ishida, T. Nakajima, Y. Honda, O. Kitao, H. Nakai, T. Vreven, J. A. Montgomery, Jr., J. E. Peralta, F. Ogliaro, M. Bearpark, J. J. Heyd, E. Brothers, K. N. Kudin, V. N. Staroverov, R. Kobayashi, J. Normand, K. Raghavachari, A. Rendell, J. C. Burant, S. S. Iyengar, J. Tomasi, M. Cossi, N. Rega, J. M. Millam, M. Klene, J. E. Knox, J. B. Cross, V. Bakken, C. Adamo, J. Jaramillo, R. Gomperts, R. E. Stratmann, O. Yazyev, A. J. Austin, R. Cammi, C. Pomelli, J. W. Ochterski, R. L. Martin, K. Morokuma, V. G. Zakrzewski, G. A. Voth, P. Salvador, J. J. Dannenberg, S. Dapprich, A. D. Daniels, Ö. Farkas, J. B. Foresman, J. V. Ortiz, J. Cioslowski, and D. J. Fox, *Gaussian, Inc.*, Wallingford CT, **2009**.
- <sup>29</sup> Poater, X. Fradera, M. Duran, M. Sola, *Chem. Eur. J.*, 2003, **9**, 400.
- <sup>30</sup> E. Matito, M. Duran, M. Sola, *J. Chem. Phys.*, 2005, **122**, 014109.

- <sup>31</sup> (a) R. F. W. Bader, *Atoms in Molecules: A Quantum Theory*, Clarendon Press, Oxford, **1990**. (b) C. F. Matta, R. J. Boyd, (Ed.), *The Quantum Theory of Atoms in Molecules*, Wiley-VCH Verlag, **2007**.
- <sup>32</sup> R. F. W. Bader, T. T. Nguyen-Dang, *Adv. Quantum Chem.*, 1981, **14**, 63.
- <sup>33</sup> A. D. Becke, *J. Chem. Phys.*, 1988, **88**, 2547.
- <sup>34</sup> (a) E. Matito, P. Salvador, M. Duran, M. Solà, *J. Phys. Chem. A*, 2005, **110**, 5108. (b) E. Mattio, P. Salvador, M. Duran, M. Solà, *J. Phys. Chem.*, 2006, **110**, 5108.
- <sup>35</sup> T. Lu, F. Chen, *J. Comp. Chem.*, 2012, **33**, 580.
- <sup>36</sup> R. Herges, D. Geuenich, *J. Phys. Chem. A*, 2001, **105**, 3214.
- <sup>37</sup> T. A. Keith, R. F. W. Bader, *Chem. Phys. Lett.*, 1993, **210**, 223.
- <sup>38</sup> (a) T. M. Krygowski, H. Szatyłowicz, O. A. Stasyuk, J. Dominikowska, M. Palusiak, *Chem. Rev.*, 2014, **114**, 6383. (b) V. I. Minkin, M. N. Glukhovtsev, B. Ya. Simkin, *Aromaticity and Antiaromaticity: Electronic and Structural Aspects*; Wiley: New York, **1994**; p 313. (c) T. M. Krygowski, M. K. Cyranski, *Chem. Rev.*, 2001, **101**, 1385. (d) P. von Ragué Schleyer, H. Jiao, *Pure Appl. Chem.*, 1996, **68**, 209.
- <sup>39</sup> W. E. Barth, R. G. Lawton, *J. Am. Chem. Soc.*, 1966, **88**, 380. (b) M. Randić, N. Trinajstić, *J. Am. Chem. Soc.*, 1984, **106**, 4428. (c) G. Monaco, L. T. Scott, R. Zanasi, *J. Phys. Chem. A*, 2008, **112**, 8136. (d) A. M. Orendt, J. C. Facelli, S. Bai, A. Rai, M. Gossett, L. T. Scott, J. Boerio-Goates, R. J. Pugmire, D. M. Grant, *J. Phys. Chem. A*, 2000, **104**, 149. (e) E. Steiner, P. W. Fowler, L. W. Jenneskens, *Angew. Chem., Int. Ed.*, 2001, **40**, 362. (f) *Carbon-Rich Compounds: From Molecules to Materials*, Ed. M. M. Haley, R. R. Tykwinski, Wiley & Sons, Weinheim, **2006**. (g) *Structure, Bonding and Reactivity of Heterocyclic Compounds*, Ed. F. De Proft, P. Geerlings, Springer, **2014**.
- <sup>40</sup> H. J. Dauben, J. D. Wilson, J. L. Laiti, *J. Am. Chem. Soc.*, 1969, **91**, 1991.
- <sup>41</sup> W. H. Flygare, *Chem. Rev.*, 1974, **74**, 653.
- <sup>42</sup> (a) P. W. Fowler, E. Steiner, *Chem. Phys. Lett.*, 2002, **364**, 259. (b) A. Acocella, R. W. A. Havenith, E. Steiner, P. W. Fowler, L. W. Jenneskens, *Chem. Phys. Lett.*, 2002, **363**, 64. (c) P. W. Fowler, R. W. A. Havenith, E. Steiner, *Chem. Phys. Lett.*, 2002, **359**, 530. (d) E. Steiner, P. W. Fowler, R. W. A. Havenith, *J. Phys. Chem. A*, 2002, **106**, 7048. (e) E. Steiner, P. W. Fowler, R. G. Viglione, R. Zanasi, *Chem. Phys. Lett.*, 2002, **355**, 471. (f) A. Soncini, P. W. Fowler, I. Cernusak, E. Steiner, *Phys. Chem. Chem. Phys.*, 2001, **3**, 3920. (g) E. Steiner, P. W. Fowler, *J. Phys. Chem. A*, 2001, **105**, 9553.
- <sup>43</sup> D. Geuenich, K. Hess, F. Köhler, R. Herges, *Chem. Rev.*, 2005, **105**, 3758.